Rotational Behavior about the N3–Pyridyl Bond in 3-(Pyridin-2-yl)quinazolin-4-one and 4-Thione Derivatives

Yuxiang Wang, Yue Yang, Daiki Homma, Elsa Caytan, Christian Roussel, Azusa Sato, Hikaru Yanai, Osamu Kitagawa

Rotational Behavior about the N3−Pyridyl Bond in 3-(Pyridin-2-yl)quinazolin-4-one and 4-Thione Derivatives

Yuxiang Wang, Yue Yang, Daiki Homma, Elsa Caytan, Christian Roussel, Azusa Sato, Hikaru Yanai, and Osamu Kitagawa*

ABSTRACT: The rotational barriers about the N3−(2-pyridyl) bond in 2-*iso*-propyl-3-(pyridin-2-yl)quinazolin-4-one and the thione analogue were evaluated though VT-NMR measurement of a diastereotopic *iso*-propyl group followed by a line-shape simulation. In 3-(pyridin-2-yl)quinazoline-4-thione bearing a chiral center as the C2 substituent, the formation of dynamic diastereomers was detected by NMR. The rotational pathway about the N3−(2-pyridyl) bond and the stereochemistries of dynamic diastereomers were revealed through a computational study.

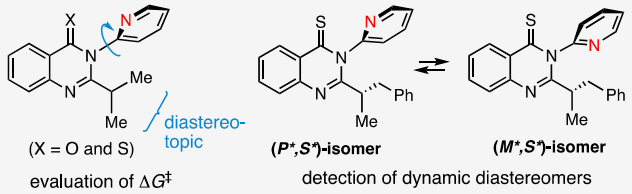

3-Arylquinazolin-4-ones have been known to possess diverse biological activities.[1] For example, 2-methyl derivatives **I** and **II** bearing 2-tolyl and 2-chlorophenyl groups at the N3 atom have been used as a hypnotic-sedative drug (methaqualone) and tranquilizer (mecroqualone), respectively (Figure 1).[1a,c] In addition, it has been reported that methaqualone **I** and mecroqualone **II** possess atropisomers (enantiomers) owing to the rotational restriction around the N3−Ar bond, and the atropisomers have different pharmacological activities.[1a] Thus, the rotational stability about the N3−Ar bond in quinazolin-4-one derivatives bearing an *ortho*-substituted phenyl group as the N3 substituent has significance in terms of both structural organic chemistry and medicinal chemistry.

We recently reported the rotational stability of 3-aryl quinazolin-4-ones (thiones) **III**−**V** bearing a minimal *ortho*-substituent (Figure 1).[2,3] In 2-fluorophenyl derivatives **III**, the atropisomers could be isolated at ambient temperature ($\Delta G^{\ddagger}$ = 26.1−26.5 kcal mol^{-1}, half-lives of racemization of 8.7−17 days),[2,4] while those of 2-deuteriophenyl derivatives **IV** and **V** could not be separated because of the lower rotational barrier (20−23 kcal mol^{-1}).[3] On the other hand, although bioactive quinazolin-4-one derivatives **VI** and **VII** bearing the 2-pyridyl group are also known,[5] the rotational behavior about the N3−(2-pyridyl) bond has not been explored. The steric size of the 2-pyridyl group is smaller than that of a simple phenyl group; hence, it may be difficult to evaluate the rotational stability about the N3−(2-pyridyl) bond. Indeed, there is little research on the rotational behavior of a bond around a simple 2-pyridyl group.[6]

Since the 2-pyridyl group has also been widely used as a directing group for C−H activation in the field of synthetic organic chemistry,[7] we were curious about the rotational behavior around the N3−(2-pyridyl) bond. In this Note, we report the rotational barriers and pathways of the N3−(2-pyridyl) bond in 2-*iso*-propyl-3-(pyridin-2-yl)quinazolin-4-one and 4-thione derivatives. Furthermore, the detection of dynamic diastereomers in 3-(pyridin-2-yl)quinazoline-4-thione bearing a chiral center as a C2 substituent and the stereochemical assignment are also described.

Several 2-alkylated-3-(pyridin-2-yl)quinazolin-4-ones **1a**−**d** and their thione analogues **2a**−**d** were prepared in accordance with Scheme 1,[8] and their NMR measurements were conducted in $CDCl_3$. In the ^{1}H NMR spectrum of 2-ethyl-3-(pyridin-2-yl)quinazolin-4-one **1a**, a considerable broadening of CH_2 hydrogens was observed (other hydrogens except for the CH_2 gave sharp NMR signals, see SI), while the CH_2 hydrogens of quinazoline-4-thione **2a** converted from quinazolinone **1a** showed sharp and nonequivalent NMR signals (Figure 2). This result indicates that in thione **2a** the atropisomerism (axial chirality) due to the rotational restriction around the N3−(2-pyridyl) bond arises at the NMR time scale and CH_2 hydrogens become diastereotopic.

Also, in the ^{1}H NMR spectra of 2-(*iso*-propyl)quinazolinone **1b** and the thione analogue **2b**, behavior similar to that of 2-ethyl derivatives **1a** and **2a** was observed. That is, two Me groups in quinazolinone **1b** were observed as a broad signal, while those in quinazolin-thione **2b** showed sharp and nonequivalent doublet signals (Figure 3a).

A variable-temperature nuclear magnetic resonance (VT-NMR) spectroscopy experiment using *iso*-propyl derivatives **1b**

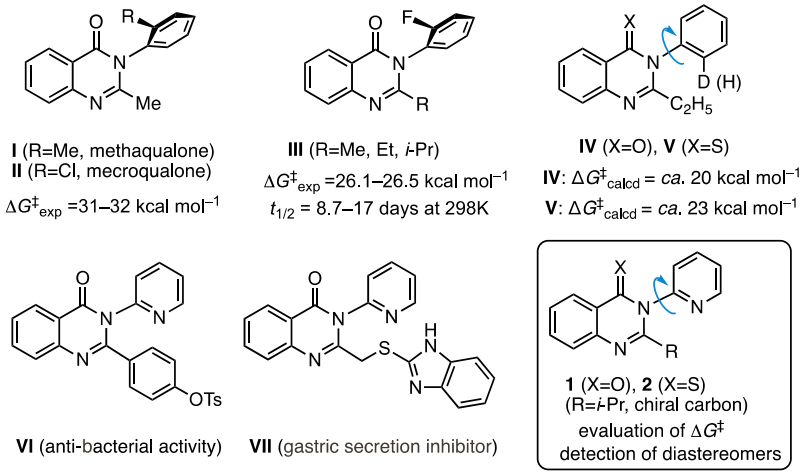

Figure 1. Various 3-arylquinazolin-4-one (thione) derivatives and their rotational stability.

Scheme 1. Synthesis of 2-Alkylated-3-(pyridin-2-yl)quinazolin-4-ones 1a–d and the Thione Analogues 2a–d[a]

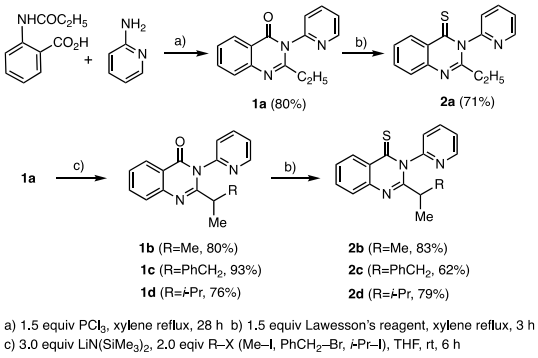

[a](a) 1.5 equiv of PCl_3, xylene ruflex, 28 h. (b) 1.5 equiv Lawesson's reagent, xylene reflux, 3 h. (c) 3.0 equiv of $LiN(siMe_3)_2$, 2.0 eqiv of R–X (Me–I, $PhCH_2$–Br, *i*-Pr–I), THF, rt, 6 h.

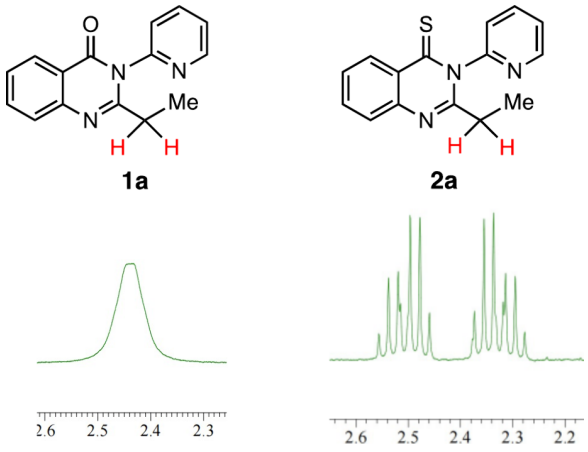

Figure 2. ^{1}H NMR signals of CH_2 hydrogens (Ha, Hb) in **1a** and **2a** at rt in $CDCl_3$.

and **2b**, which gave simple doublet signals, was further investigated. VT-NMR signals of two Me groups in **1b** and **2b** in $CDCl_2$–$CDCl_2$ are shown in Figure 3b. Hydrogens of the Me group in quinazolinone **1b**, which were detected as a broad singlet signal at around room temperature (300 K),

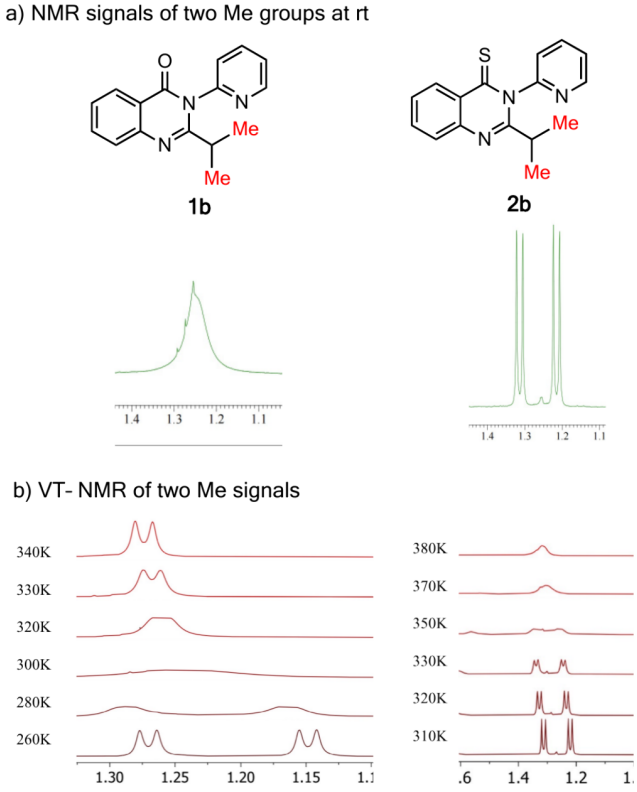

Figure 3. (a) ^{1}H NMR signals of two Me hydrogens in **1b** and **2b** at rt in $CDCl_3$. (b) VT-NMR spectra of **1b** and **2b** in $CDCl_2$–$CDCl_2$.

gradually became sharp with increasing temperature, and a clear doublet coupling was observed around 330 K, while a decrease in temperature led to the nonequivalency of two Me hydrogens (280 K). Me hydrogens of quinazoline-thione **1b**, which showed sharp and nonequivalent doublet signals around rt (300 K), broadened with increasing temperature and coalesced around 370 K.

On the basis of the VT-NMR spectra of **1b** and **2b**, a line-shape simulation with the WinDNMR program was conducted to evaluate the rotational barriers around the N3–(2-pyridyl) bond (see the SI). As a result, the rotational barriers in **1b** and **2b** were calculated to be 14.5 and 17.9 kcal mol^{-1}, respectively (Figure 4).

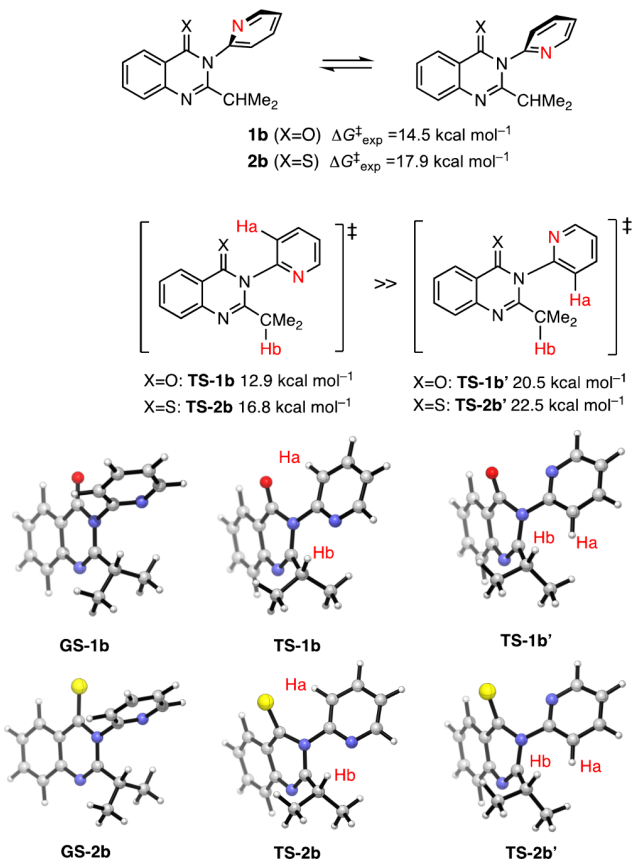

Figure 4. Rotational barriers about the N3−(2-pyridyl) bond and consideration of the rotational pathway through DFT calculations using PCM($CHCl_3$)-B3LYP/cc-pVDZ.

To elucidate the rotational pathway about the N3−(2-pyridyl) bond, a computational study was performed (Figure 4). In the most stable ground-state structures **GS-1b** and **GS-2b** that were evaluated by DFT calculations [PCM($CHCl_3$)-B3LYP/cc-pVDZ], the pyridyl group was almost perpendicular toward the quinazolinone plane (the twist angles in **1b** and **2b** are 78.7 and 85.5°, respectively). Furthermore, it was found that the rotational pathways **TS-1b** and **TS-2b** in which the pyridine nitrogen passes through the *iso*-propyl side are highly advantageous in comparison with the pathways **TS-1b′** and **TS-2b′** in which the pyridine nitrogen passes through the C═O (C═S) side (the activation energies for **TS-1b** and **TS-2b** are 7.6 and 5.7 kcal mol^{-1} lower than those of **TS-1b′** and **TS-2b′**, respectively). The calculated rotational barrier values (12.9 and 16.8 kcal mol^{-1}) also correlated well with the experimental values (14.5 and 17.9 kcal mol^{-1}). Such favorable passing of the N atom from the *iso*-propyl side via **TS-1b** or **TS-2b** is supported by NBO[9] and QTAIM[10] calculations (for full details, see the Supporting Information). That is, electrostatic interactions in the X···Ha−C and N···Hb−C moieties effectively stabilize in **TS-1b** and **TS-2b**.

We expected that the addition of protic acid to **1b** would lead to a decrease in the rotational barrier (acid-accelerated molecular rotor) and a change in the rotational pathway through the formation of intramolecular hydrogen bonds (N^+—H···O═C).[11] Unfortunately, the protonation of the pyridine nitrogen resulted in the decomposition of the quinazolinone ring.[12]

^{1}H NMR spectra of 2-(1-phenylpropan-2-yl)-3-(pyridin-2-yl)quinazolinone **1c** and thione **2c** (racemate) bearing a chiral center as the C2 substituent were subsequently measured in $CDCl_3$. In quinazolinone **1c**, a remarkable broadening of all signals was observed. On the other hand, quinazolinethione **2c** showed sharp signals. Interestingly, in **2c**, the formation of two sets of signals was observed. For example, two kinds of Me hydrogens were detected in a ratio of 2.2:1 at 1.45 and 1.21 ppm, respectively (Figure 5). The formation of two sets of

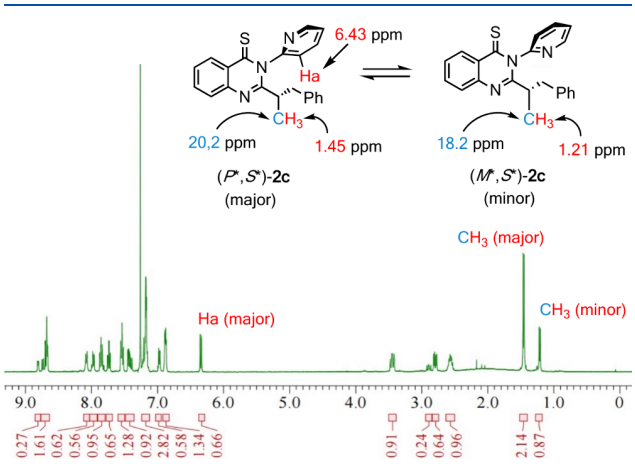

Figure 5. ^{1}H NMR spectrum of 3-(pyridin-2-yl)quinazoline-4-thione **2c** at rt in $CDCl_3$.

signals in **2c** was also observed in the ^{13}C NMR spectrum, and these were probably due to the diastereomers based on the chiral carbon and dynamic atropisomerism about the N3−(2-pyridyl) bond. In the major diastereomer, an aromatic hydrogen was observed at a considerably high magnetic field (6.43 ppm) in comparison with other aromatic hydrogens. We predicted that this aromatic hydrogen is the C3 hydrogen Ha on the pyridine ring and that the high field shift is due to the anisotropic effect of the benzene ring of the benzyl group.[3]

Our prediction was supported by a computational study. During structural optimization of **2c**, four stable conformers, which are shown in Figure 6, were found [the relative energies of the other conformers were higher than 2.5 kcal mol^{-1} in comparison with the most stable conformer (*P**,*S**)-**2c-2**]. Two conformers possess a (*P**,*S**)-configuration, while the other two conformers possess a (*M**,*S**)-configuration. The Boltzmann distribution of the considered conformers indicates that (*P**,*S**)-**2c** and (*M**,*S**)-**2c** exist in a ratio of 2.3:1, and this ratio correlated very well with the integrated ratio (2.2:1) of the two Me hydrogens in ^{1}H NMR.

Among the four conformers, the molecular geometries of two conformers (*P**,*S**)-**2c-2** and (*M**,*S**)-**2c-2**, which implied $\pi-\pi$ stacking between the pyridine and benzene rings, suggested notable anisotropic effects on the ^{1}H NMR chemical shifts. In the GIAO calculation using the PBE0 hybrid functional, the Ha atom in (*P**,*S**)-**2c-2** was computed at the high field side (6.64 ppm).[13] In contrast, the Ha atom of (*M**,*S**)-**2c-2** was in the normal range for hydrogens on an aromatic ring (7.34 ppm). The simulated chemical shifts of Ha in (*P**,*S**)-**2c** and (*M**,*S**)-**2c** involving also the contribution of nonstacking conformer **2c-1** were evaluated to be 6.94 and 7.43 ppm, respectively. Moreover, the chemical shifts of Me hydrogens in (*P**,*S**)-**2c** and (*M**,*S**)-**2c** were simulated to be 1.24 and 1.07 ppm, respectively. Although the simulated values

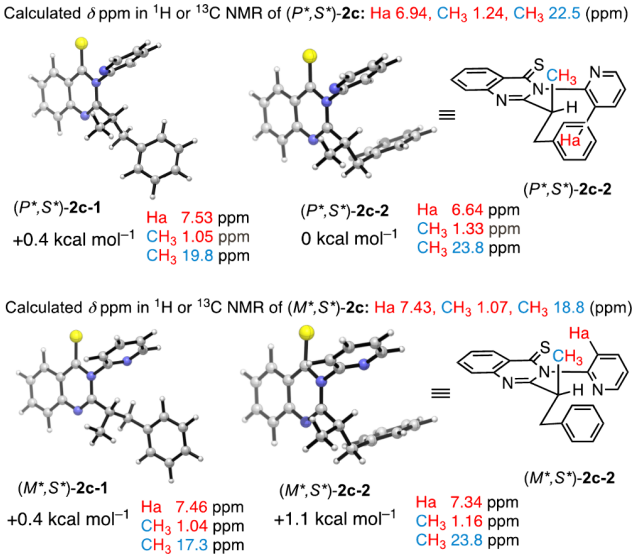

Figure 6. Stable conformers of **2c** and the chemical shifts of Ha and CH_3 groups evaluated by DFT calculations using PCM($CHCl_3$)-B3LYP/cc-pVDZ.

differ somewhat from the values detected via ^{1}H NMR [Ha in (*P**,*S**)-**2c** at 6.43 ppm, Me in (*P**,*S**)-**2c** and (*M**,*S**)-**2c** at 1.45 and 1.21 ppm, respectively], the trend of chemical shifts correlated well between the simulation and experiment. The simulated chemical shifts (22.5 and 18.8 ppm, Figure 6) of the CH_3 carbon in (*P**,*S**)-**2c** and (*M**,*S**)-**2c** also correlated well with the chemical shifts (20.2 and 18.2 ppm, respectively, Figure 5) detected in ^{13}C NMR. On the basis of these results, the stereochemistries of major and minor diastereomers, which were detected in ^{1}H NMR, were determined to be the (*P**,*S**) and (*M**,*S**) configurations, respectively.

The formation of dynamic diastereomers based on a chiral carbon and unstable atropisomerism was also observed in the ^{1}H NMR spectrum of 2-(3-methylbutan-2yl)-3-(pyridin-2-yl)quinazoline-4-thiones **2d** (racemate). In **2d** bearing the *iso*-propyl group, the diastereomers were detected in a ratio of 1.5:1 (Figure 7), while an upfield shift of pyridine hydrogen Ha observed in benzyl derivative **2c** was not found (see SI).

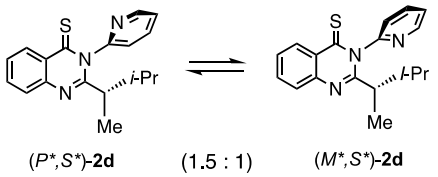

Figure 7. Dynamic diastereomers observed in *iso*-propyl derivative **2d**.

In conclusion, we succeeded in the evaluation of the rotational barriers about the N3−(2-pyridyl) bond in 2-(*iso*-propyl)-3-(pyridin-2yl)quinazolin-4-one and 4-thione derivatives through VT-NMR measurement of diastereotopic Me groups followed by a line-shape simulation. Furthermore, the rotational pathway about the N3−(2-pyridyl) bond was revealed by the DFT study. In 3-(pyridin-2-yl)quinazoline-4-thione bearing a chiral center as the C2 substituent, the formation of diastereomers based on a chiral carbon and dynamic atropisomerism around the N3−(2-pyridyl) bond was detected in NMR, and the stereochemistries of dynamic diastereomers were determined through the simulation using the DFT method.

EXPERIMENTAL SECTION

Melting points were recorded on a melting point apparatus and are uncorrected. ^{1}H and ^{13}C NMR spectra were recorded on 400 and 101 MHz spectrometer. Chemical shifts δ were given in ppm, and coupling constants J were given in Hz. ^{1}H and ^{13}C NMR chemical shifts were determined by using residual signals of the deuterated solvent, $CDCl_3$ (^{1}H, δ 7.26 ppm; ^{13}C, δ 77.01 ppm). HRMS spectra were recorded on a double focusing magnetic sector mass spectrometer using an ESI-TOF. Column chromatography was performed on silica gel (75−150 μm). Medium-pressure liquid chromatography (MPLC) was performed on a 25 × 4 cm i.d. prepacked column (silica gel, 10 μm) with a UV detector.

2-Ethyl-3-(pyridin-2-yl)quinazolin-4(3*H*)-one (1a). Under a N_2 atmosphere, to *N*-propionyl anthranilic acid (386 mg, 2.0 mmol) and 2-aminopyridine (565 mg, 6.0 mmol) in xylene (10 mL) was added PCl_3 (0.26 mL, 3.0 mmol). The mixture was stirred for 8 h at 130 °C (oil bath) and then for 15 h at 80 °C (oil bath). The mixture was poured into saturated aqueous $NaHCO_3$ and extracted with AcOEt. The AcOEt extracts were washed with brine and dried over $MgSO_4$. Purification of the residue by column chromatography (hexane/AcOEt = 1:1) gave **1a** (403 mg, 80%). **1a**: white solid; mp 100−101 °C; IR (neat) 1668.5 cm^{-1}; ^{1}H NMR (400 MHz, $CDCl_3$) δ 8.71 (1H, dd, J = 4.8, 0.8 Hz), 8.27 (1H, d, J = 8.0 Hz), 7.95 (1H, td, J = 7.6, 2.0 Hz), 7.72−7.79 (2H, m), 7.44−7.48 (2H, m), 7.40 (1H, d, J = 8.0 Hz), 2.43 (2H, brs), 1.23 (3H, t, J = 7.2 Hz); ^{13}C{^{1}H} NMR (101 MHz, $CDCl_3$) δ 162.5, 157.0, 151.0, 150.2, 147.8, 138.9, 134.7, 127.3, 127.0, 126.7, 124.5, 124.1, 120.9, 28.9, 11.0; MS (ESI-TOF) m/z [MNa]$^+$ 274; HRMS (ESI-TOF) m/z [MNa]$^+$ Calcd for $C_{15}H_{13}N_3NaO$ 274.0956, found 274.0970.

2-Ethyl-3-(pyridin-2-yl)quinazoline-4(3*H*)-thione (2a). Under a N_2 atmosphere, a mixture of **1a** (503 mg, 2.0 mmol) and Lawesson's reagent (1.213 g, 3.0 mmol) in xylene (8 mL) was stirred for 3 h at 150 °C (oil bath). The mixture was poured into water and extracted with AcOEt. The AcOEt extracts were washed with brine, dried over $MgSO_4$, and evaporated to dryness. Purification of the residue by column chromatography (hexane/AcOEt = 1:1) gave **2a** (380 mg, 71%). **2a**: yellow solid; mp 102−104 °C; IR (neat) 1597 cm^{-1}; ^{1}H NMR (400 MHz, $CDCl_3$) δ 8.73−8.77 (2H, m), 7.96 (1H, td, J = 7.8, 1.6 Hz), 7.79 (1H, td, J = 8.0, 1.2 Hz), 7.73 (1H, dd, J = 8.4, 1.2 Hz), 7.47−7.52 (2H, m), 7.38 (1H, d, J = 8.0 Hz), 2.50 (1H, dq, J = 16.8, 7.2 Hz), 2.32 (1H, dq, J = 16.8, 7.2 Hz), 1.26 (3H, t, J = 7.2 Hz); ^{13}C{^{1}H} NMR (101 MHz, $CDCl_3$) δ 190.1, 156.1, 154.5, 150.5, 142.8, 139.0, 135.1, 130.8, 128.8, 128.02, 127.98, 124.6, 124.1, 29.6, 11.1; MS (ESI-TOF) m/z [MH]$^+$ 268; HRMS (ESI-TOF) m/z [MH]$^+$ Calcd for $C_{15}H_{14}N_3S$ 268.0908, found 268.0918.

2-*iso*-Propyl-3-(pyridin-2-yl)quinazolin-4(3*H*)-one (1b). Under a N_2 atmosphere, to **1a** (363 mg, 1.44 mmol) in THF (7 mL) was added lithium hexamethyldisilazide (LiHMDS, 1 M THF solution, 4.3 mL, 4.3 mmol). After being stirred for 1 h at rt, to the mixture was added CH_3I (0.18 mL, 2.8 mmol), and then the mixture was stirred for 5 h at rt. The mixture was poured into saturated aqueous NH_4Cl and extracted with AcOEt. The AcOEt extracts were washed with brine, dried over $MgSO_4$, and evaporated to dryness. Purification of the residue by column chromatography (hexane/AcOEt = 1:1) gave **1b** (306 mg, 80%). **1b**: white solid; mp 111−112°; IR (neat) 1684 cm^{-1}; ^{1}H NMR (400 MHz, $CDCl_3$) δ 8.71 (1H, dq, J = 4.9, 0.8 Hz), 8.26 (1H, dq, J = 8.1, 0.8 Hz), 7.94 (1H, td, J = 7.8, 1.6 Hz), 7.71−7.78 (2H, m), 7.43−7.48 (2H, m), 7.40 (1H, dt, J = 8.0, 1.2 Hz), 2.51 (1H, sept, J = 6.8 Hz), 1.27 (6H, brs); ^{13}C{^{1}H} NMR (101 MHz, $CDCl_3$) δ 162.8, 160.8, 151.2, 150.2, 147.9, 138.8, 134.6, 127.4, 127.0, 126.6, 124.4, 124.2, 120.9, 32.7, 21.2; MS (ESI-TOF) m/z [MH]$^+$ 266; HRMS (ESI-TOF) m/z [MH]$^+$ Calcd for $C_{16}H_{16}N_3O$ 266.1293, found 266.1287.

2-*iso*-Propyl-3-(pyridin-2-yl)quinazoline-4(3*H*)-thione (2b). **2b** was prepared from **1b** (133 mg, 0.5 mmol) in accordance with the experimental procedure for the synthesis of **2a**. Purification of the

residue by column chromatography (hexane/AcOEt = 3:1) gave **2b** (116 mg, 83%). **2b**: yellow solid; mp 115−117 °C; IR (neat) 1586 cm^{-1}; ^1H NMR (400 MHz, $CDCl_3$) δ 8.72−8.77 (2H, m), 7.95 (1H, td, J = 7.6, 1.6 Hz), 7.72−7.81 (2H, m), 7.46−7.51 (2H, m), 7.38 (1H, dt, J = 8.0, 1.2 Hz), 2.47 (1H, sept, J = 6.8 Hz), 1.31 (3H, d, J = 6.4 Hz), 1.22 (3H, d, J = 6.8 Hz); $^{13}C\{^1H\}$ NMR (101 MHz, $CDCl_3$) δ 190.2, 160.1, 154.6, 150.4, 143.0, 138.8, 135.0, 130.8, 128.8, 128.0, 127.9, 124.5, 124.2, 33.6, 21.5, 21.4; MS (ESI-TOF) m/z $[MH]^+$ 282; HRMS (ESI-TOF) m/z $[MH]^+$ Calcd for $C_{16}H_{16}N_3S$ 282.1065, found 282.1088.

2-(1-Phenylpropan-2-yl)-3-(pyridin-2-yl)quinazolin-4(3*H*)-one (1c). Under N_2 atmosphere, to **1a** (503 mg, 2 mmol) in THF (7 mL) was added lithium hexamethyldisilazide (LiHMDS, 1 M THF solution, 4 mL, 4 mmol). After the mixture was stirred for 1 h at rt, $PhCH_2Br$ (0.48 mL, 4 mmol) was added, and then the mixture was stirred for 3 h at rt. The mixture was poured into saturated aqueous NH_4Cl and extracted with AcOEt. The AcOEt extracts were washed with brine, dried over $MgSO_4$, and evaporated to dryness. Purification of the residue by column chromatography (hexane/AcOEt = 1:1) gave **1c** (635 mg, 93%). **1c**: orange oil; IR (neat) 1680 cm^{-1}; ^1H NMR (400 MHz, $CDCl_3$) δ 8.68 (1H, brs), 8.29 (1 H, d, J = 7.6 Hz), 7.76−7.83 (3H, m), 7.31−7.50 (2.5H, m), 7.16−7.22 (3H, m), 6.90 (2H, brs), 6.50 (0.5H, brs), 3.29 (1H, brs), 2.74 (1H, m), 2.61 (1H, m), 1.37 (3H, brs); $^{13}C\{^1H\}$ NMR (101 MHz, $CDCl_3$) δ 162.5, 159.6, 150.9, 150.0, 147.7, 139.8, 138.6, 134.6, 129.0, 128.3, 127.2, 126.9, 126.6, 126.3, 124.3, 124.2, 120.7, 42.3, 40.7, 19.4; MS (ESI-TOF) m/z $[MNa]^+$ 364; HRMS (ESI-TOF) m/z $[MNa]^+$ Calcd for $C_{22}H_{19}N_3NaO$ 364.1426, found 364.1409.

2-(1-Phenylpropan-2-yl)-3-(pyridin-2-yl)quinazoline-4(3*H*)-thione (2c). **2c** was prepared from **1c** (581 mg, 1.7 mmol) in accordance with the experimental procedure for the synthesis of **2a**. Purification of the residue by column chromatography (hexane/AcOEt = 10:1) gave a residue of **2c** (376 mg, 62%). **2c**: yellow solid; mp 153−156 °C; IR (neat) 1589 cm^{-1}; ^1H NMR (400 MHz, $CDCl_3$) δ 8.81 (0.33H, dd, J = 4.2, 1.2 Hz), 8.74 (0.33H, dd, J = 8.4, 1.2 Hz), 8.66−8.70 (1.33H, m), 8.08 (0.66H, d, J = 8 Hz), 7.96−8.00 (0.66H, m), 7.81−7.88 (1H, m), 7.74 (0.66H, td, J = 7.8, 1.6 Hz), 7.52−7.56 (1.33H, m), 7.37−7.45 (1H, m), 7.14−7.26 (3H, m), 6.96−7.00 (0.66H, m), 6.87−6.89 (1.33H, m), 6.34 (0.66H, d, J = 8.4 Hz), 3.42−3.48 (1H, m), 2.89 (0.33H, dd, J = 13.6, 10.0 Hz), 2.80 (0.66H, dd, J = 13.6, 5.6 Hz), 2.53−2.59 (1H, m), 1.46 (2H, d, J = 6.8 Hz), 1.22 (1H, d, J = 6.8 Hz); $^{13}C\{^1H\}$ NMR (101 MHz, $CDCl_3$) δ 190.2, 189.8, 159.0, 158.9, 154.5, 154.2, 150.4, 150.2, 142.9, 142.8, 139.8, 139.6, 139.0, 138.5, 135.0, 130.8, 129.11, 129.05, 128.8, 128.7, 128.5, 128.3, 128.0, 127.9, 126.5, 126.3, 124.7, 124.4, 124.3, 42.4, 42.0, 41.2, 40.6, 20.2, 18.2; MS (ESI-TOF) m/z $[MNa]^+$ 380; HRMS (ESI-TOF) m/z $[MNa]^+$ Calcd for $C_{22}H_{19}N_3NaS$ 380.1197, found 380.1203.

2-(3-Methylbutan-2yl)-3-(pyridin-2-yl)quinazolin-4(3*H*)-one (1d). **1d** was prepared from **1a** (1.03 g, 4.1 mmol) and Me_2CHI (0.8 mL, 8 mmol) in accordance with the experimental procedure for the synthesis of **1b**. Purification of the residue by column chromatography (hexane/AcOEt = 1:1) gave **1d** (913 mg, 76%). **1d**: white solid; mp 147−148 °C; IR (neat) 1680 cm^{-1}; ^1H NMR (400 MHz, $CDCl_3$) δ 8.70 (1H, d, J = 3.6 Hz), 8.26 (1H, m), 7.93 (1H, td, J = 7.6, 1.6 Hz), 7.69−7.75 (2H, m), 7.41−7.48 (2H, m), 7.35 (1H, d, J = 8.0 Hz), 2.16 (1H, brs), 1.96 (1H, quint, J = 7.2 Hz), 1.23 (3H, brs), 0.86 (3H, d, J = 6.8 Hz), 0.79 (3H, brs); $^{13}C\{^1H\}$ NMR (101 MHz, $CDCl_3$) δ 162.8, 160.5, 151.4, 150.3, 148.0, 138.7, 134.6, 127.4, 126.9, 126.5, 124.3, 120.8, 45.0, 32.3, 21.9, 19.2, 16.8; MS (ESI-TOF) m/z $[MNa]^+$ 316; HRMS (ESI-TOF) m/z $[MNa]^+$ Calcd for $C_{18}H_{19}N_3NaO$ 316.1426, found 316.1438.

2-(3-Methylbutan-2yl)-3-(pyridin-2-yl)quinazoline-4(3*H*)-thione (2d). **2d** was prepared from **1d** (147 mg, 0.5 mmol) in accordance with the experimental procedure for synthesis of **2a**. Purification of the residue by column chromatography (hexane/AcOEt = 5:1) gave **2d** (122 mg, 79%). **2d**: yellow solid; mp 109−111 °C; IR (neat) 1587 cm^{-1}; ^1H NMR (400 MHz, $CDCl_3$) δ 8.71−8.77 (2H, m), 7.93 (1H, t, J = 7.6 Hz), 7.71−7.80 (2H, m), 7.46−7.50 (2H, m), 7.34 (1H, t, J = 9.2 Hz), 2.15−2.32 (1H, m), 1.87−1.99 (1H, m), 1.27 (1.8H, d, J = 6.4 Hz), 1.16 (1.2H, d, J = 6.8 Hz), 0.87−0.83 (4.2H, m), 0.77 (1.8H, d, J = 6.8 Hz); $^{13}C\{^1H\}$ NMR (101 MHz, $CDCl_3$) δ 190.13, 190.05, 159.9, 159.8, 154.8, 154.6, 150.4, 150.3, 142.9, 142.8, 139.0, 138.6, 135.00, 134.97, 130.7, 128.69, 128.65, 128.0, 127.9, 124.7, 124.4, 123.8, 46.2, 45.4, 32.7, 32.2, 22.0, 21.9, 19.3, 18.9, 17.2, 16.9; MS (ESI-TOF) m/z $[MH]^+$ 310; HRMS (ESI-TOF) m/z $[MH]^+$ Calcd for $C_{18}H_{20}N_3S$ 310.1378, found 310.1375.

AUTHOR INFORMATION

Corresponding Author

Osamu Kitagawa − *Chemistry and Materials Program, College of Engineering, Shibaura Institute of Technology, Tokyo 135-8548, Japan;* orcid.org/0000-0001-7964-1879; Email: kitagawa@shibaura-it.ac.jp

Authors

Yuxiang Wang − *Chemistry and Materials Program, College of Engineering, Shibaura Institute of Technology, Tokyo 135-8548, Japan*

Yue Yang − *Chemistry and Materials Program, College of Engineering, Shibaura Institute of Technology, Tokyo 135-8548, Japan*

Daiki Homma − *Chemistry and Materials Program, College of Engineering, Shibaura Institute of Technology, Tokyo 135-8548, Japan*

Elsa Caytan − *Univ Rennes, CNRS, ISCR−UMR 6226, F-35000 Rennes, France;* orcid.org/0000-0003-0490-3074

Christian Roussel − *Aix Marseille Université, Centrale Marseille, CNRS, iSm2 UMR 7313, 13397 Cedex 20 Marseille, France*

Azusa Sato − *School of Pharmacy, Tokyo University of Pharmacy and Life Sciences, Tokyo 192-0392, Japan*

Hikaru Yanai − *School of Pharmacy, Tokyo University of Pharmacy and Life Sciences, Tokyo 192-0392, Japan;* orcid.org/0000-0003-4638-5113

Complete contact information is available at: https://pubs.acs.org/10.1021/acs.joc.4c01186

Notes

The authors declare no competing financial interest.

ACKNOWLEDGMENTS

This work was partly supported by JSPS KAKENHI (C 23K04755).

REFERENCES

(1) Representative papers on bioactive 3-arylquinazolin-4-one derivatives: (a) Mannschreck, A.; Koller, H.; Stühler, G.; Davis, M. A.; Traber, J. The Enantiomers of Methaqualone and their Unequal Anticonvulsive Activity. *Eur. J. Med. Chem. Chim. Ther.* **1984**, *19*, 381−383. (b) Chenard, B. L.; Welch, W. M.; Blake, J. F.; Butler, T.

W.; Reinhold, A.; Ewing, F. E.; Menniti, F. S.; Pagnozzi, M. Quinazolin-4-one α-Amino-3-hydroxy-5-methyl-4-isoxazolepropionic Acid (AMPA) Receptor Antagonists: Structure−Activity Relationship of the C-2 Side Chain Tether. *J. J. Med. Chem.* **2001**, *44*, 1710−1717. (c) Dolma, S.; Lessnick, S. L.; Hahn, W. C.; Stockwell, B. R. Identification of genotype-selective antitumor agents using synthetic lethal chemical screening in engineered human tumor cells. *Cancer Cell* **2003**, *3*, 285−296. (d) Dixit, R.; Mehta, H.; Dixit, B. Synthesis, characterization and antimicrobial studies of new 2-(2-chloroquinolin-3-yl)-3-(substituted phenyl/pyridinyl)quinazolin-4(3H)-one derivatives using L-proline as a catalyst. *Med. Chem. Res.* **2015**, *24*, 773−786. (e) Ghosh, S. K.; Nagarajan, R. Deep eutectic solvent mediated synthesis of quinazolinones and dihydroquinazolinones: synthesis of natural products and drugs. *RSC Adv.* **2016**, *6*, 27378−27387. (f) Bouley, R.; Ding, D.; Peng, Z.; Bastian, M.; Lastochkin, E.; Song, W.; Suckow, M. A.; Schroeder, V. A.; Wolter, W. R.; Mobashery, S.; Chang, M. Structure−Activity Relationship for the 4(3H)-Quinazolinone Antibacterials. *J. Med. Chem.* **2016**, *59*, 5011−5021. (g) Lodola, A.; Bertolini, S.; Biagetti, M.; Capacchi, S.; Facchinetti, F.; Gallo, P. M.; Pappani, A.; Mor, M.; Pala, D.; Rivara, S.; Visentini, F.; Corsi, M.; Capelli, A. M. Atropisomerism and Conformational Equilibria: Impact on PI3Kδ Inhibition of 2-((6-Amino-9H-purin-9-yl)methyl)-5-methyl-3-(o-tolyl)quinazolin-4(3H)-one (IC87114) and Its Conformationally Restricted Analogs. *J. Med. Chem.* **2017**, *60*, 4304−4315. (h) Qian, Y.; Allegretta, G.; Janardhanan, J.; Peng, Z.; Mahasenan, K. V.; Lastochkin, E.; Gozun, M. M. N.; tejera, S.; Schroeder, V. A.; Wolter, R.; Feltzer, R.; Mobashery, S.; Chang, M. Exploration of the Structural Space in 4(3H)-Quinazolinone Antibacterials. *J. Med. Chem.* **2020**, *63*, 5287−5296.

(2) Iida, A.; Matsuoka, M.; Hasegawa, H.; Vanthuyne, N.; Farran, D.; Roussel, C.; Kitagawa, O. N−C Axially Chiral Compounds with an ortho-Fluoro Substituent and Steric Discrimination between Hydrogen and Fluorine Atoms Based on a Diastereoselective Model Reaction. *J. Org. Chem.* **2019**, *84*, 3169−3175.

(3) Saito, K.; Miwa, S.; Iida, A.; Fujimoto, Y.; Caytan, E.; Roussel, C.; Kitagawa, O. Detection of Isotopic Atropisomerism Based on ortho-H/D Discrimination. *Org. Lett.* **2021**, *23*, 7492−7496.

(4) Hakgor, A.; Gunal, S. E. Energy barriers to rotation in axially chiral quinazolin-4-ones. *Tetrahedron* **2021**, *100*, No. 132506.

(5) (a) Patil, A.; Ganguly, S.; Surana, S. Synthesis and antiulcer activity of 2-[5-substituted-1-H-benzo(d) imidazol-2-yl sulfinyl]-methyl-3-substituted quinazoline-4-(3H) ones. *J. Chem. Sci.* **2010**, *122*, 443−450. (b) Habib, O. M. O.; Hassan, H. M.; El-Meka, A. Studies on Some Benzoxazine-4-one Derivatives with Potential Biological Activity. *Am. J. Org. Chem.* **2012**, *2*, 45−51.

(6) (a) Huth, S. E.; Stone, E. A.; Crotti, S.; Miller, S. J. On the Ability of the N−O Bond to Support a Stable Stereogenic Axis: Peptide-Catalyzed Atroposelective N-Oxidation. *J. Org. Chem.* **2023**, *88*, 12857−12862. (b) Clayden, J.; Fletcher, S. P.; McDouall, J. J. W.; Rowbottom, J. M. Controlling Axial Conformation in 2-Arylpyridines and 1-Arylisoquinolines: Application to the Asymmetric Synthesis of QUINAP by Dynamic Thermodynamic Resolution. *J. Am. Chem. Soc.* **2009**, *131*, 5331−5343. (c) Osmialowski, B.; Kolehmainen, E.; Dobosz, R.; Gawinecki, R.; Kauppinen, R.; Valkonen, A.; Koivukorpi, J.; Rissanen, K. Self-Organization of 2-Acylaminopyridines in the Solid State and in Solution. *J. Phys. Chem. A.* **2010**, *114*, 10421−10426.

(7) (a) Chatani, N.; Ie, Y.; Kakiuchi, F.; Murai, S. $Ru_3(CO)_{12}$-Catalyzed Reaction of Pyridylbenzenes with Carbon Monoxide and Olefins. Carbonylation at a C−H Bond in the Benzene Ring. *J. Org. Chem.* **1997**, *62*, 2604−2610. (b) Park, Y. J.; Park, J.-W.; Jun, C.-H. Metal−Organic Cooperative Catalysis in C−H and C−C Bond Activation and Its Concurrent Recovery. *Acc. Chem. Res.* **2008**, *41*, 222−234. (c) Neufeldt, S. R.; Sanford, M. S. Controlling Site Selectivity in Palladium-Catalyzed C−H Bond Functionalization. *Acc. Chem. Res.* **2012**, *45*, 936−946. (d) Tiwari, V. K.; Kamal, T.; Kapur, M. Ruthenium-Catalyzed Heteroatom-Directed Regioselective C−H Arylation of Indoles Using a Removable Tether. *Org. Lett.* **2015**, *17*, 1766−1769. (e) Kakiuchi, F.; Kochi, T. Chelation-Assisted Catalytic C-C, C-Si, and C-Halogen Bond Formation by Substitution via the Cleavage of $C(sp^2)$-H and $C(sp^3)$-H Bonds. *J. Synth. Org. Chem,. Jpn.* **2015**, *73*, 1099−1110.

(8) (a) Matsuoka, M.; Goto, M.; Wzorek, A.; Soloshonok, V. A.; Kitagawa, O. Diastereoselective α-Alkylation of Metallo Enamines Generated from N-C axially Chiral Mebroqualone Derivatives. *Org. Lett.* **2017**, *19*, 2650−2653. (b) Niijima, E.; Imai, T.; Suzuki, H.; Fujimoto, Y.; Kitagawa, O. Thionation of Optically Pure N-C Axially Chiral Quinazolin-4-one Derivatives with Lawesson's Reagent. *J. Org. Chem.* **2021**, *86*, 709−715.

(9) Weinhold, F.; Landis, C. R. *Valency and Bonding: A Natural Bond Orbital Donor−Acceptor Perspective*; Cambridge University Press: Cambridge, UK, 2005.

(10) (a) *The Quantum Theory of Atoms in Molecules*; Matta, C. F., Boyd, R. J., Eds.; Wiley-VCH, 2007. (b) Bader, R. F. W. *Atoms in Molecules: A Quantum Theory*; Clarendon Press: Oxford, UK, 1990.

(11) Typical papers on protic acid-mediated molecular rotors: (a) Dial, B. E.; Pellechia, P. J.; Smith, M. D.; Shimizu, K. D. Proton Grease: An Acid Accelerated Molecular Rotor. *J. Am. Chem. Soc.* **2012**, *134*, 3675−3678. (b) Suzuki, Y.; Kageyama, M.; Morisawa, R.; Dobashi, Y.; Hasegawa, H.; Yokojima, S.; Kitagawa, O. Synthesis of optically active N-C axially chiral tetrahydroquinoline and its response to acid-accelerated molecular rotor. *Chem. Commun.* **2015**, *51*, 11229−11232. (c) Wu, Y.; Wang, G.; Li, Q.; Xiang, J.; Jiang, H.; Wang, Y. A multistage rotational speed changing molecular rotor regulated by pH and metal cations. *Nat. Commun.* **2018**, *9*, 1953.

(12) Perreault, S.; Chandrasekhar, J.; Patel, L. Atropisomerism in Drug Discovery: A Medicinal Chemistry Perspective Inspired by Atropisomeric Class I PI3K Inhibitors *Acc. Chem. Res.* **2022**, *55*, 2581−2593.

(13) Geometry optimizations were carried out by using the widespread B3LYP density functional. For the NMR prediction, the PBE0 functional was reported to give better results, see: Adamo, C.; Barone, V. Toward chemical accuracy in the computation of NMR shieldings: the PBE0 model. *Chem. Phys. Lett.* **1998**, *298*, 113−119.